RAPID COMMUNICATIONS

PHYSICAL REVIEW C VOLUME 43, NUMBER 5 MAY 1991

Tracking the dissipation of energy and angular momentum in central collisions between Ag and ^{40}Ar of 7, 17, 27, and 34 MeV/nucleon

T. Ethvignot,[1,2] A. Elmaani,[1] N. N. Ajitanand,[1] J. M. Alexander,[1] E. Bauge,[1,2] P. Bier,[1] L. Kowalski,[1] M. T. Magda,[1] P. Désesquelles,[2] H. Elhage,[2] A. Giorni,[2] D. Heuer,[2] S. Kox,[2] A. Lleres,[2] F. Merchez,[2] C. Morand,[2] D. Rebreyend,[2] P. Stassi,[2] J. B. Viano,[2] S. Benrachi,[3] B. Chambon,[3] B. Cheynis,[3] D. Drain,[3] and C. Pastor[3]

[1]*State University of New York at Stony Brook, Stony Brook, New York 11794-3400*

[2]*Institut des Sciences Nucléaires de Grenoble, Université Joseph Fourier and Institut National de Physique Nucléaire et de Physique des Particules, 53, Avenue des Martyrs, 38026, Grenoble CEDEX, France*

[3]*Institut de Physique Nucléaire de Lyon, Université Claude Bernard I and Institut National de Physique Nucléaire et de Physique des Particules, 43, Boulevard du 11 Novembre 1918, Villeurbanne CEDEX, France*

(Received 18 January 1991)

A 4π charged-particle multidetector has been used to study the reaction ^{40}Ar+^{nat}Ag from 280–1356 MeV. Charged-particle multiplicity distributions show a low-multiplicity group associated with peripheral collisions and a high-multiplicity group associated with central collisions. Average multiplicities for central collisions increase with increasing projectile energy, indicating ever-increasing collision violence. Angular distributions of emitted protons are essentially isotropic for $\theta \gtrsim 80°$ in a reference frame characterized by the empirical systematics of linear momentum transfer (i.e., $\approx 100\%$ to $\approx 70\%$ from 7–34 MeV/nucleon). Spectra of these protons at side angles are evaporationlike in shape and indicate relative effective temperatures of 3, 6, 8, and 12 MeV for beam energies of 7, 17, 27, and 34A MeV, respectively. Azimuthal angular correlations between various particle pairs are consistent with spin-driven emission from emitter sources of reasonable spin values. In short, these results support a classical picture of extensively thermalized emitter nuclei even for initial excitation energies of ≈ 5 MeV per system nucleon and spins of $\gtrsim 100\hbar$.

It is known that heavy projectiles such as ^{40}Ar dissipate a great deal of energy in central nuclear collisions.[1] Fusion reactions (complete and/or incomplete) have been observed at energies up to $E/A \approx 30$ MeV (e.g., Refs. 2-4), but a saturation of the neutron-emission multiplicities for $E/A \gtrsim 30$ MeV suggests a limit in the energy deposition for higher energies.[5] In this work we used the AMPHORA multidetector array[6] to study energy and angular momentum deposition in central collisions of ^{40}Ar (E/A =7, 17, 27, and 34 MeV) with ^{nat}Ag. Charged-particle multiplicities are used to monitor the gross energy deposition or collision violence. Angular and energy distributions of the protons are used to monitor the energy thermalization, and azimuthal angular correlations reflect the angular momenta.

The experiment was performed at the Système Accélérateur Rhône-Alpes SARA by a collaboration from Grenoble, Lyon, and Stony Brook. The AMPHORA array is made up of 140 CsI detectors that cover $\approx 80\%$ of 4π sr.[6] Crystals of CsI are located with cylindrical symmetry around the beam in two parts: (a) the ball with 92 trapezoidal units in a set of seven crown rings covering polar angles from $\theta = 15°$ to 164° and (b) the wall with 48 hexagonal units covering 2°–15°. Particle identification by pulse-shape analysis is unique for H and He isotopes; additional groups can also be identified, such as Li fragments ($Z=3$) and all other fragments of $Z \geq 4$. Proton energy spectra at $\theta \approx 67°$ ($\Delta\theta \approx 20°$) were calibrated by reference to a companion experiment that used small Si telescopes ($\theta = 65°$) for the ^{40}Ar+^{nat}Ag reaction (E/A =17 MeV).[3] Data analysis has exploited the DALI package from Grenoble[7] supplemented by a variety of output programs and reaction simulations from Stony Brook.[8,9]

Figure 1 shows multiplicity distributions for charged particles and fragments (CP) from the reaction with E/A =27 MeV. For "all reactions" (AMPHORA enabled by ball multiplicity > 1), this distribution seems to break into two groups, a peak of high multiplicity and a shoulder of lower multiplicities. The multiplicity of the light charged particles (LCP) H and He is also shown in Fig. 1 for three separate situations. For all the reactions recorded, LCP (all), there is a very broad distribution of $M_{\mathrm{H,He}}$ with no clear break between peripheral and central collisions. However, a coincidence trigger for peripheral reactions, e.g., a projectilelike fragment at $\approx 4°$, is associated with the low-multiplicity group. (Note that the peripheral collisions were suppressed to some degree by the enabling condition.) Coincidence triggers of ^{4}He at large angles, e.g., at 67°, are associated with the high-multiplicity group and can, therefore, be used to select central collisions; if Li fragments are used as a trigger, the results are very similar to those shown for ^{4}He. In fact, these (and other similar) central-collision triggers are not particularly dependent on angle. As shown for Li fragments in Fig. 2, the patterns of average multiplicities

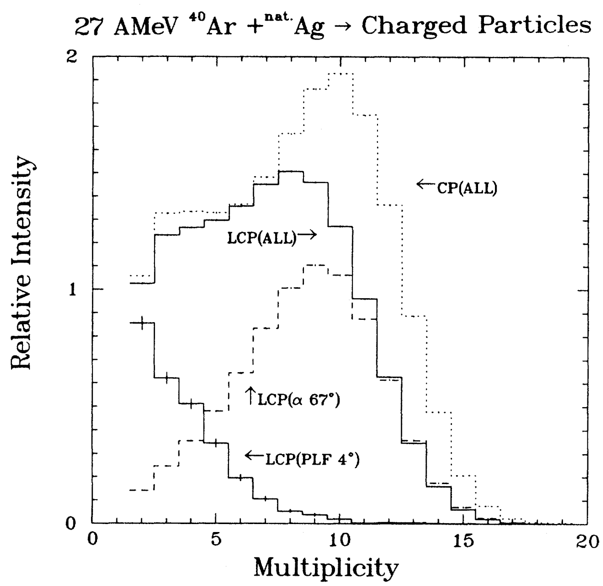

FIG. 1. Multiplicity distributions for charged particles and fragments (CP) and for light charged particles (LCP) of $Z=1$ and 2. The short-dashed histogram is for CP from all reactions enabled by $M>1$ in the AMPHORA ball; the upper solid one is for LCP. The lower two histograms show LCP multiplicities triggered by a projectilelike fragment (PLF) at 4° and an α particle at 67° (typical of peripheral and central collisions, respectively). In Figs. 1–3 the distributions are uncorrected for detection efficiency. Error bars give statistical uncertainties.

are very similar, even for angles of 10°–70°, and indicate an association with large energy depositions. This angular range is $\approx 40°-140°$ for ^{1}H or ^{4}He.

As an indicator for energy dissipation in central collisions, we have chosen average H and He multiplicities $\langle M\rangle_{\text{H,He}}$ in coincidence with a Li trigger fragment at 47°. Figure 3 shows a steady increase of these average multiplicities (and associated energy deposition) with

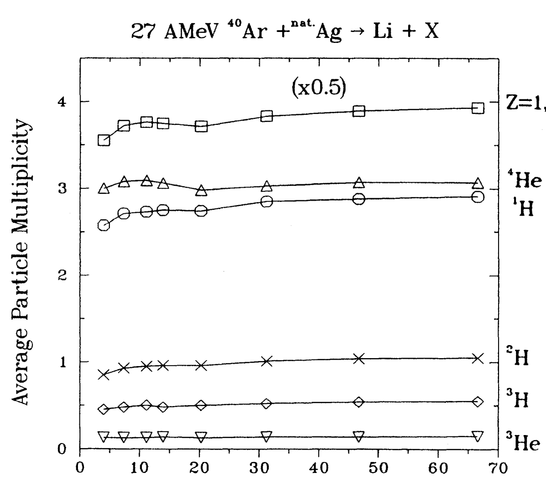

FIG. 2. Average multiplicities gated by Li fragments at various angles.

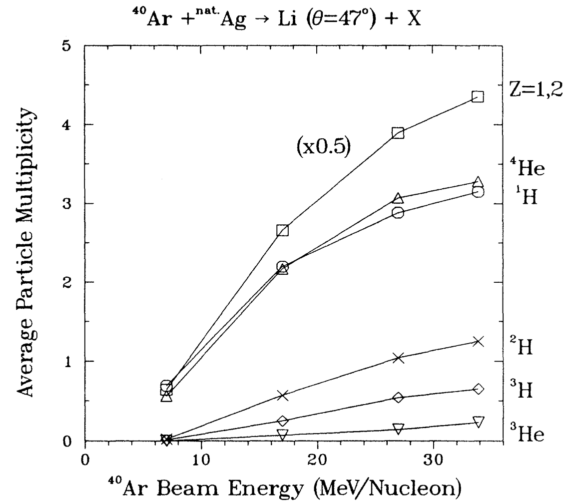

FIG. 3. Average multiplicities gated by Li fragments for different beam energies.

incident energy from E/A of 7–34 MeV; a slight hint for the approach to multiplicity saturation is given, however, by the decreasing slopes of the curves. To get a feeling for the extent of energy thermalization, we show proton angular and energy distributions in Figs. 4 and 5. In Figs. 4(a) and 5(a), results are given in the laboratory system and in Figs. 4(b) and 5(b) in the average emitter frame. Emitter velocities were taken from the trend of measurements of the linear momentum transfer (LMT): LMT equals 100%, 90%, 80%, and 70% for $E/A=7$, 17, 27, and 34 MeV, respectively.[2–4] For Fig. 4(b) the data were transformed with the average emitter-frame velocities of ^{1}H from Fig. 5. The results of the

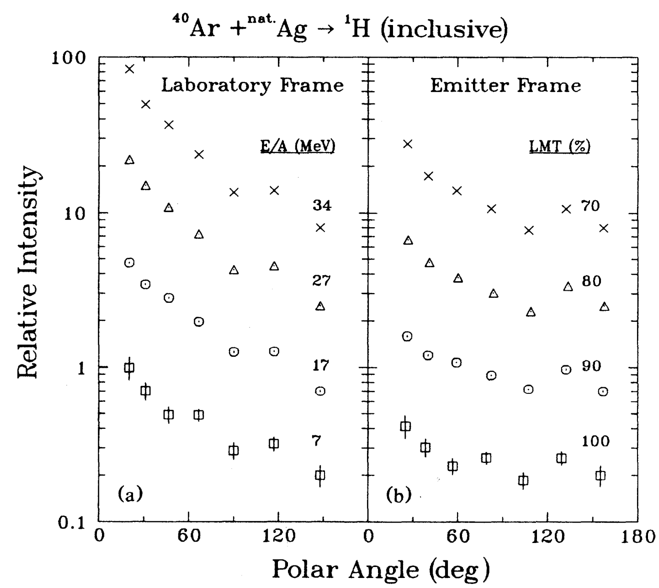

FIG. 4. Inclusive proton angular distributions $d\sigma/d\Omega$ (arbitrary units) in (a) the laboratory and (b) the emitter frames. The beam energy is indicated along with the value of the linear momentum transfer (LMT) (Refs. 2–4).

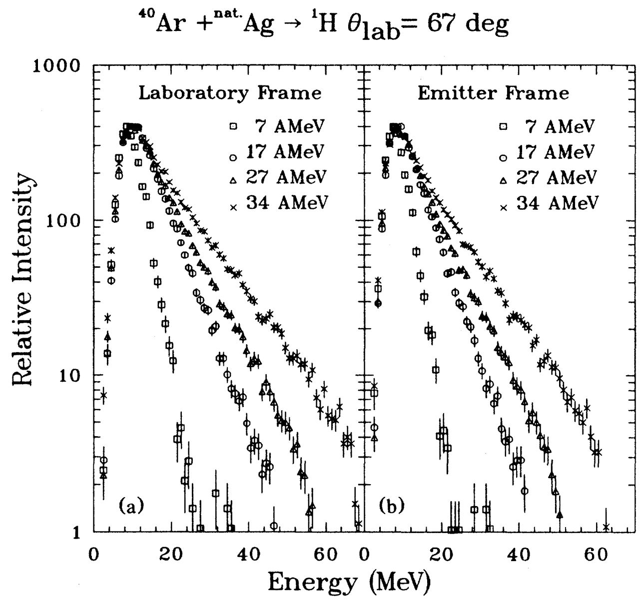

FIG. 5. Inclusive proton energy distributions in (a) the laboratory and (b) the emitter frames, LMT as in Fig. 4. High-energy spectral slopes are ≈ 3, 6, 8, and 12 MeV, respectively.

calculations and transformations would be changed only slightly by an error of $\pm 10\%$ in the value of LMT or the emitter-frame velocity.

In Fig. 4 we see that the proton emission is isotropic for emitter angles of $\gtrsim 80°$, consistent with fusion into a hot emitter nucleus. Similarly, the energy distributions in Fig. 5 show evaporationlike spectra consistent with spectral slopes or relative effective temperatures gradually increasing from ≈ 3 to 12 MeV. This classic pattern for fusionlike reactions, which has been established for beam energies of $E/A = 7$ and 17 MeV,[2,3] seems to persist even to E/A of 27 and 34 MeV and initial excitations of ≈ 700 MeV or ≈ 5 MeV per nucleon in the emitter nucleus. Analysis of the velocity distributions of evaporation residues leads to the same conclusion.[4] This is not to say that the excited nuclear object has achieved complete thermal equilibrium, and indeed the spectral shapes may be breaking into two components for $E/A = 34$ MeV. However, this does indicate extensive collisional energy mixing toward thermalization. The patterns of Figs. 4 and 5 are essentially unchanged by requiring a Li trigger fragment as in Fig. 3.

The role of angular momentum in these emitter nuclei can be studied by azimuthal angular distributions or correlations between emitted particles.[2,10] Figure 6 shows a selection of such azimuthal angular correlations for ^{4}He-X pairs. Let us first look at the qualitative aspects of these data. They all have maxima at 0° and 180°, minima at 90°, and show essentially no preference for 0° or 180°. The ratio of 180° to 90° becomes more pronounced with increasing ejectile mass and with decreasing incident energy. There is no change in this qualitative pattern from 7 to 34A MeV, as might be expected if the mechanism changes. This is just the pattern expected for evaporation from a thermalized composite nucleus, i.e., favored emission perpendicular to the emitter spin; for this mechanism the strength of the anisotropy is related to the parameter β_2, the average rotational or spin-off energy of an ejectile at the emitter surface divided by the temperature.[2,11] Since heavier ejectiles have more spin-off energy, they have larger anisotropies. Dependence of the anisotropy (ratio of 180° to 90°) on incident energy is more complex than its dependence on mass because both

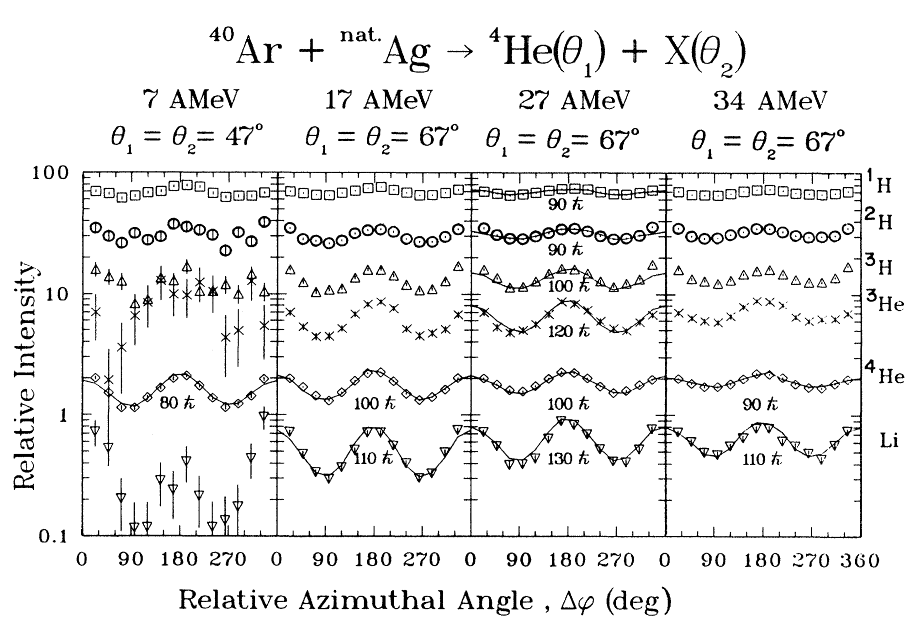

FIG. 6. Azimuthal angular correlations (θ and $\Delta\phi$ in the laboratory frame) for ^{4}He-X pairs for the cases indicated. For each curve the calculations use LMT values given in the text, effective excitation energies of $\frac{2}{3}$ the maximum possible,[2] and spin zones from zero to the J_{max} value indicated.

emitter spin (or rotational energy) and temperature can be expected to change with the beam energy. The effective temperature is surely increased with energy, as shown in Figs. 3–5, and this will weaken the anisotropies; however, the average emitter spin may be increased as well, and this will strengthen the anisotropies.

To get a feeling for the interplay between these driving forces, we have made a series of reaction simulations with the code COULGAN.[8,9] These calculations consider only two effective steps of an evaporation cascade (as described in Ref. 2), and vary only the composite nucleus spin range in attempting to fit the data (i.e., minimizing differences for $90° < \Delta\phi < 270°$ for steps of $10\hbar$ in $J_{\max}$). The smooth curves in the figures give results from these simulations with triangular spin distributions from 0 to $J_{\max}$. A value of $80\hbar$ is required for $J_{\max}$ from α-α correlations at $7A$ MeV; this is consistent with earlier measurements of the out-of-plane correlations.[2] Fits to the α-α data at 17, 27, and $34A$ MeV give $J_{\max}$ values that are somewhat larger. The correlations at $27A$ MeV for the ^1H or ^2H ejectiles seem to indicate slightly smaller spins compared to the heavier Li ejectiles. The cross sections for central collisions (e.g., for CP multiplicities of ≥ 7 in Fig. 1) indicate incident partial waves of 0 to $\approx 200\hbar$; this tells us that there are, indeed, large angular momenta involved in these reactions. Our purpose in this initial study is simply to indicate that these data can indeed be described by reasonable spin zones if the ejectiles arise from rotating, evaporationlike emitters.

The azimuthal distributions given in Fig. 6 were obtained at large angles where extensive energy thermalization is indicated by the angular and energy distributions shown in Figs. 4 and 5. At more forward angles, one notes forward peaking of the angular distribution and can expect that a single composite nuclear emitter will probably not give an adequate model. Figure 7 shows ^{4}He-^{4}He azimuthal correlations for a series of angles. One can generally account for these distributions for the larger angles by small variations in the effective spins of the emitters, but for $\theta = 21°$ one cannot fit the ratio of $\Delta\phi$ for $24°/168°$. Probably fragment breakup (e.g., ^{8}Be) and/or strong prethermalization emission dominate and alter the character of these correlations at small angles.

It is quite interesting that the statistical-model framework is able to describe these azimuthal correlations for such a large range of angles and incident energies. Probably the emitters are too excited to actually achieve complete thermal equilibrium, but the success of the statistical procedure may well not demand such equilibration. Pre-equilibrium models for collisional energy mixing are also based on phase-space dominance. As this mixing progresses and particles escape, their correlations may also be driven by the available phase space as embodied in the state density of the residual nucleus. This condition of phase-space control during the collision cascade might be satisfied more easily than the condition of complete equilibration.

There is special incentive for trying to understand the emission of Li fragments; a problem of great current concern is the attempt to distinguish sequential fragment emission from instantaneous multifragmentation. In Fig. 8 we show azimuthal angular correlations for Li-X pairs. The strength of these correlations increases with ejectile mass and decreases with angle in just the way discussed above for evaporationlike emission. In fact, our statistical-model simulations, shown by the smooth curves,

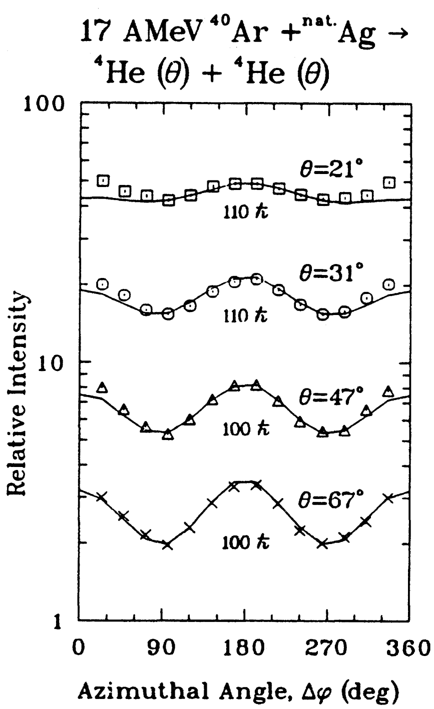

FIG. 7. Azimuthal angular correlations for ^{4}He-^{4}He pairs for the cases indicated. Curves were calculated as described for Fig. 6.

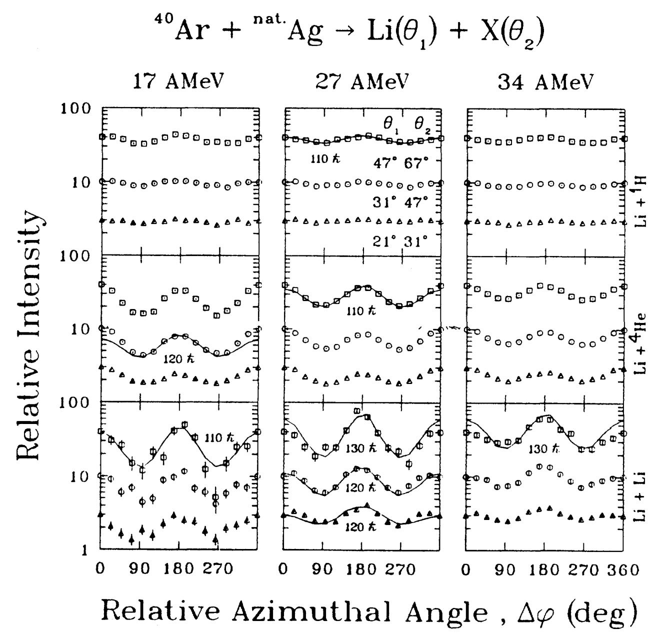

FIG. 8. Azimuthal angular correlations for Li-X pairs for the cases indicated. Curves were calculated as described for Fig. 6.

follow these major trends. However, there are two interesting deviations from the simulations: (a) For Li-^{4}He pairs the observed ratios of 0°/180° are often somewhat greater than those calculated. (b) For Li-Li pairs ($E/A=27$ and 34 MeV) the observed ratios for 0°/180° are often less than those calculated. One is tempted to conclude that the major driving force for Li ejection is indeed the phase space of the emitter unit, but that there are some additional perturbations. The excess emission at 0° for Li-He pairs might arise from the formation and breakup of excited states of ^{11}B, a process that has been identified in small-angle correlation studies.[12] Any fragment breakup in more peripheral collisions could give a similar effect. The deficit of emission at 0° for Li-Li pairs might arise from Coulomb repulsion between two fragments emitted very close together in both time and space.[8-10,13,14] We have made simulation calculations of this latter effect by following classical trajectories of Li fragments with an exponential distribution of time delays.[8,9] Preliminary results for the incident energies of 27 and 34A MeV suggest that the average time interval between two Li emissions is $\lesssim 10^{-21}$ s.

We can summarize this study as follows: (a) Charged-particle multiplicities for central collisions increase with incident ^{40}Ar energy from 7 to 34A MeV indicating an ever increasing energy dissipation. (b) Proton energy and angular distributions indicate extensive thermalization of this energy. (c) Azimuthal angular correlations between particle pairs indicate extensive deposition of angular momentum and its role in the available phase space. (d) Pairs of Li-Li fragments are essentially consistent with statistically driven emission with perturbations due to mean time delays of $\lesssim 10^{-21}$ s. (e) The combined evidence suggests that one has made highly excited nuclei with initial excitations of up to ≈ 5 MeV per emitter nucleon and spins of $\gtrsim 100\hbar$. Since we know that the average nuclear binding energy is only ≈ 8 MeV, it seems amazing that a statistically driven composite system can continue to function at such extremely high excitations and spins.

Financial support has been provided by the United States Department of Energy and the Centre National de la Recherche Scientifique of France. T.E. is also grateful to the Société Lyonaise de Banque for partial support.

[1] J. Galin, in *Proceedings of the XXIst Summer School on Nuclear Physics, Mikolajki, Poland, 1990,* IOP Conf. Proc. (Institute of Physics and Physical Society, London, in press) [Grand Accèlèrateur National d'Ions Lourds (GANIL) Report, 1990, p. 90-17].

[2] R. Lacey *et al.*, Phys. Rev. C **37**, 2540 (1988).

[3] C. J. Gelderloos, J. M. Alexander, J. Boger, P. DeYoung, A. Elmaani, M. T. Magda, A. Narayanan, and J. Sarafa (unpublished).

[4] A. Lleres, Ph.D. thesis, Institut des Sciences Nucléaires de Grenoble, 1988.

[5] D. X. Jiang *et al.*, Nucl. Phys. A **503**, 560 (1989).

[6] D. Drain *et al.*, Nucl. Instrum. Methods Phys. Res. Sect. A **281**, 528 (1989).

[7] D. Heuer and A. Lleres (private communication).

[8] N. N. Ajitanand and J. M. Alexander (unpublished). The codes MODGAN and COULGAN originate from GANES, N. N. Ajitanand, R. Lacey, G. F. Peaslee, E. Duek, and J. M. Alexander, Nucl. Instrum. Methods Phys. Res. Sect. A **243**, 111 (1986).

[9] A. Elmaani, N. N. Ajitanand, T. Ethvignot, and J. M. Alexander (unpublished). The code MENEKA is an extensive outgrowth of KALLIOPI, R. L. McGrath, A. Elmaani, J. M. Alexander, P. A. DeYoung, T. Ethvignot, M. S. Gordon, and E. Renshaw, Comput. Phys. Commun. **59**, 507 (1990).

[10] A. Elmaani *et al.*, in *Corinne 90,* Proceedings of the International Workshop on Particle Correlations and Interferometry in Nuclear Collisions, Nantes, France, 1990, edited by D. Ardouin (World Scientific, Singapore, 1990), p. 154; A. Giorni *et al.*, *ibid.*, p. 437.

[11] N. N. Ajitanand, G. LaRana, R. Lacey, L. C. Vaz, G. F. Peaslee, D. M. de Castro Rizzo, M. Kaplan, and J. M. Alexander, Phys. Rev. C **34**, 877 (1986).

[12] J. Pochodzalla *et al.*, Phys. Rev. C **35**, 1695 (1987).

[13] P. A. DeYoung *et al.*, Phys. Rev. C **41**, R1885 (1990).

[14] R. Trockel *et al.*, Phys. Rev. Lett. **59**, 2844 (1987).